

Using microfluidic devices to study thrombosis in pathological blood flows

Bradley A. Herbig, Xinren Yu, and Scott L. Diamond^{a)}

Department of Chemical and Biomolecular Engineering, Institute for Medicine and Engineering, 1024 Vagelos Research Laboratory, University of Pennsylvania, Philadelphia, Pennsylvania 19104, USA

(Received 8 January 2018; accepted 23 February 2018; published online 15 May 2018)

Extreme flows can exist within pathological vessel geometries or mechanical assist devices which create complex forces and lead to thrombogenic problems associated with disease. Turbulence and boundary layer separation are difficult to obtain in microfluidics due to the low Reynolds number flow in small channels. However, elongational flows, extreme shear rates and stresses, and stagnation point flows are possible using microfluidics and small perfusion volumes. In this review, a series of microfluidic devices used to study pathological blood flows are described. In an extreme stenosis channel pre-coated with fibrillar collagen that rapidly narrows from 500 μm to 15 μm , the plasma von Willebrand Factor (VWF) will elongate and assemble into thick fiber bundles on the collagen. Using a micropost-impingement device, plasma flow impinging on the micropost generates strong elongational and wall shear stresses that trigger the growth of a VWF bundle around the post (no collagen required). Using a stagnation-point device to mimic the zone near flow reattachment, blood can be directly impinged upon a procoagulant surface of collagen and the tissue factor. Clots formed at the stagnation point of flow impingement have a classic core-shell architecture where the core is highly activated (P-selectin positive platelets and fibrin rich). Finally, within occlusive clots that fill a microchannel, the Darcy flow driven by $\Delta P/L > 70 \text{ mm-Hg/mm-clot}$ is sufficient to drive NETosis of entrapped neutrophils, an event not requiring either thrombin or fibrin. Novel microfluidic devices are powerful tools to access physical environments that exist in human disease. *Published by AIP Publishing.*

<https://doi.org/10.1063/1.5021769>

INTRODUCTION

Extreme pathological blood flows are both an important contributor to and a result of thrombosis. Thrombosis is the pathological clotting of blood within the lumen of a vessel and is driven primarily by two processes: coagulation and platelet adhesion. Coagulation is the protein reaction cascade initialized by either/both exposure to the tissue factor (TF) or/and a negatively charged surface (contact activation), resulting in the formation of thrombin. Thrombin is able to both activate platelets via PAR1/4 and cleave fibrinogen to enable its polymerization into fibrin, which both contribute to thrombus formation and stability. Platelet adhesion is driven by platelet activation in response to thrombin and/or shear and occurs through multiple integrins on the platelet surface. GPIb, $\alpha_{\text{IIb}}\beta_3$, and GPVI all play a role in stable platelet binding to fibrin, collagen, and the von Willebrand factor (VWF) to aggregate platelets into a clot.

In the context of pathological flows, VWF plays a particularly important role in platelet adhesion at high shear rates. VWF is a protein that circulates in multimerized form and aggregates under exposure to high shear rates. When it binds to the surface of a platelet thrombus via GPIb or to collagen at high shear, additional platelets can roll on VWF via GPIb and firmly

^{a)} Author to whom correspondence should be addressed: sld@seas.upenn.edu. Tel.: 215-573-5702.

bind via $\alpha_{IIb}\beta_3$. This interaction can enhance the formation of thrombi under high shear conditions, potentially leading to vessel occlusion.

For the purposes of this review, pathological flows can be defined as where the blood either reaches wall shear rates of $>5000\text{ s}^{-1}$ or where recirculation and stagnation points cause transport limitations for blood components. They can occur in and exacerbate numerous diseases such as coronary artery disease, stroke, and atherosclerosis and in medical devices such as left ventricular assist devices (LVADs) and mechanical heart valves. For example, the unusual pressure gradient created in stagnation point regions has been correlated with the development of atherosclerotic plaques.¹ Building a better understanding of the hemodynamics in these diseases is crucial to developing better treatments and designing better medical devices in the future.

One particularly useful platform for studying the extreme blood flows discussed above is microfluidics. The vast array of microfluidic devices that have been developed and utilized has been useful in many fields. Microfluidic devices are particularly useful for studying extreme blood flows for their operational flexibility, control of fluid shear, and control of flow geometry. In this review, a discussion of these advantages is demonstrated through examples of the use of microfluidics to study thrombosis in pathological flows.

OPERATIONAL FLEXIBILITY

Microfluidics has been utilized extensively to design robust experiments to better understand biological mechanisms under conditions of fluid flow. This platform technology is particularly useful operationally because of its ease of use, versatility, scale, and control of fluid conditions.

Ease of design and fabrication

The design and manufacturing of microfluidic devices are well-developed and extensively described. The overall process is straightforward and allows for customization of device features and design iteration at relatively low costs.

Device features are designed in computer-aided design (CAD) programs (e.g., DraftSight or AutoCAD), which are then made into photomasks at a printing company (e.g., OutputCity). Using these custom photomasks, the device features are transferred onto silicon wafers using standard photolithography.² The resulting silicon wafers can then be used as a reusable master mold to create polydimethylsiloxane (PDMS) microfluidic devices. These devices are made by degassing the PDMS prepolymer and curing reagents and curing them over the master wafer at 65°C for 3 h. The temperature and time used depend on the design of the microfluidic devices, as high temperatures tend to shrink some features. Lower curing temperatures (45°C) and longer curing times (24 h) followed by curing at higher temperatures can be used for devices with more exact features.³ After cooling, the molded PDMS can then be peeled off, cut into individual devices (if the initial design includes multiple devices per mask), and modified with appropriate hole-punches to create the inlets, outlets, and other ports in the final device. Because microfluidic devices used to study pathological flows often contain complex geometries, the ease of fabrication enables an iterative approach to device design and experimental design.

Ease of detection

Another operational advantage of using microfluidic devices to study thrombosis in pathological flows is the ease with which spatiotemporal changes in the clot structure and composition can be observed using a fluorescent microscope. Common fluorophores such as phycoerythrin (PE), allophycocyanin (APC), and fluorescein isothiocyanate (FITC) can be conjugated with antibodies against blood components such as CD61 (platelets), CD62P (P-selectin), fibrin, or VWF to fluorescently track thrombosis in microfluidic devices using different colors. This enables tracking of blood components and their relative concentrations in thrombi by measuring the relative intensity of the fluorescent signal throughout the clot and over time.

Scale and blood volumes

One advantage that makes microfluidics particularly suited for use in studying extreme blood flows is the relatively small volume of fluid necessary to run each experiment. Because the length scale of the channels on a microfluidic device is on the micrometer scale, even high shear experiments can be run at relatively low flow rates on the order of $\mu\text{l}/\text{min}$. Previous experimental technologies, such as parallel flow chambers, required multiple liters of blood to run an experiment with the same time length and shear rates that a couple milliliters could achieve in a microfluidic device.

Control of blood biochemistry

Microfluidics allows for significant control over blood biochemistry through the addition of a variety of anticoagulants, inhibitors, and drugs. In contrast to *in vivo* studies, where concentrations in blood are complicated by numerous factors, *in vitro* microfluidics enable precise control of the exogenous species concentration in the blood, providing insights into the mechanisms involved. Blood begins the process of coagulation as soon as it is exposed to a negatively charged surface, and so, anticoagulation is particularly important in microfluidic experiments. Numerous inhibitors of factors in the coagulation pathway, as well as reversible calcium chelators, are used.

Direct inhibition of coagulation factors is a powerful tool in microfluidic studies of pathological flows. PPACK, a direct and potent inhibitor of thrombin, is used to study the role of platelets in thrombosis without the influence of coagulation. Apixaban is a Factor Xa inhibitor which can be used to prevent the endogenous production of thrombin without inhibiting any thrombin added to the experiment exogenously. The corn trypsin inhibitor (CTI) blocks Factor XIIa and can be used at various concentrations for different effects. At a low concentration ($\sim 4 \mu\text{g}/\text{ml}$), CTI prevents the contact activation from handling of blood during the experiment but allows the formation of thrombin over a thrombotic surface, such as collagen. At a high concentration ($\sim 40 \mu\text{g}/\text{ml}$), CTI is able to fully block the intrinsic coagulation pathway, allowing the study of the extrinsic pathway.

Calcium chelators, such as sodium citrate and ethylenediaminetetraacetic acid (EDTA), prevent the calcium-dependent coagulation pathway from initiating. By adding calcium ions back into the blood (via CaCl_2 , for example) before or after introduction to the microfluidic device,⁴ coagulation can be reinitiated and clotting can proceed. Note that EDTA should only be used in platelet-free experiments because it has been shown to cause platelets to dissociate their $\alpha_{\text{IIb}}\beta_3$ integrins.⁵

Another manifestation of this advantage is in drug testing, where novel anticoagulants, anti-platelet agents, and other drug candidates can be examined for their effect on clot formation, and the dose-response relationship can be established. The number of platelets and other coagulation factors is large enough in even a small blood volume to enable statistical significance in these studies. Because overall blood volumes in microfluidic experiments are low, smaller amounts of these anticoagulants, anti-platelet agents, and other drug candidates are necessary to test their effect on platelets and/or coagulation at sufficient concentrations.

CONTROL OF FLUID SHEAR

Microfluidics allows for precise control of fluid flow and shear conditions. Because the mechanisms that dominate clotting differ between flow regimes and patterns, this ability enables microfluidics to be a powerful platform in studying how high shear pathological flows affect clot formation. Stenosis devices and impingement-post devices in particular have been useful in studying the role of VWF in high shear thrombosis.

Stenosis devices

Colace and Diamond used a stenotic-shaped microfluidic device [Fig. 1(a)] that sheared platelet-free plasma (PFP) or whole blood at pathological shear rates ($>30\,000 \text{ s}^{-1}$) and shear

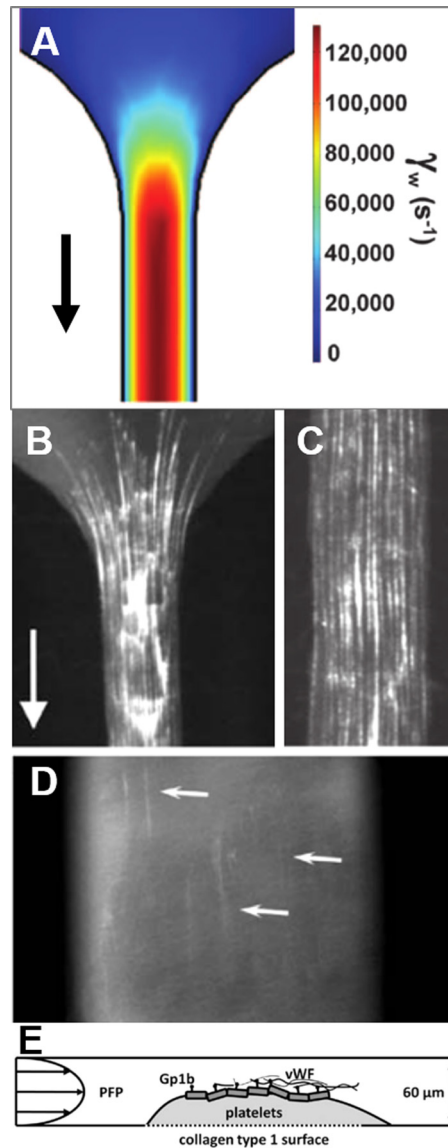


FIG. 1. VWF deposition on collagen and platelets occurs in the stenosis microfluidic device. (a) COMSOL simulation demonstrates the severe pathological wall shear rate in the stenosis device. (b) EDTA-anticoagulated platelet-free plasma (PFP) was perfused over collagen at $125\,000\text{ s}^{-1}$, resulting in the deposition of VWF fibers. (c) VWF fiber deposition on collagen was also observed in straight (non-stenotic) channels, suggesting that shear gradients are not required for VWF aggregation at extremely high shear rates. (d) A steady-state platelet clot on collagen was formed by flowing PPACK-anticoagulated whole blood at 200 s^{-1} for 1500 s, followed by perfusion of PPACK-anticoagulated PFP at $23\,400\text{ s}^{-1}$. VWF deposited in fibers on the platelet clot surface after 50 s. (e) A schematic diagram of VWF deposition in (d).

gradients over a patch of collagen to study the interactions between sheared VWF, platelets, and collagen.⁶ Unlike typical viscometry experiments, these devices allowed for single-pass perfusion of PFP or whole blood over the collagen, which allowed them to study how short (<500 ms) exposure to shear affects thrombotic potential.

In this stenosis microfluidic device, aggregation of VWF into fibers is driven by the high shear forces on plasma upstream, which causes tumbling in flow and stretches out VWF fibers to expose hydrophobic domains, which leads to lateral aggregation of VWF into fibers able to bind to the collagen surface [Fig. 1(b)]. These fibers were also observed to be fully bound to the collagen and did not relax when flow was stopped. Interestingly, the formation of VWF fibers on collagen did not require a shear gradient [Fig. 1(c)], which contrasts with previous

reports by Nesbitt *et al.*⁷ It is possible that at lower shear rates, shear gradients are more important to VWF elongation and aggregation, but Colace and colleagues found that at extreme pathological shear rates, the high shear rate was sufficient to induce VWF fiber formation on collagen. The high wall shear rate may be the dominant factor for VWF fiber bundle formation on a wall, whereas the high shear rate gradient or the elongation rate may be the critical factor for VWF bundle formation in bulk flow.

When whole blood was perfused at pathological shear rates through the device, VWF/platelet nets formed, rolled, and embolized across the collagen surface, an effect blocked by anti-GPIIb or the anti- $\alpha_{IIb}\beta_3$ inhibitor GR144053. When PPACK-anticoagulated WB was perfused and thrombi were allowed to grow to a steady state on a collagen surface at low shear, followed by high shear perfusion of PPACK-anticoagulated PFP, VWF fibers formed on the surface of the clots through platelet GPIIb [Figs. 1(d) and 1(e)]. As a result, platelet recruitment was reestablished by increasing the GPIIb/VWF tethering via increased VWF aggregation at high shear on the thrombus surface. The simple but extremely narrow stenotic channel shape over a collagen surface allowed for the capitulation of these severely pathological environments without requiring large volumes of blood.

Another common type of stenosis-shaped microfluidic device relies on a short semi-circular region blocking 20%–80% of the channel diameter to create high shear conditions and observe the resulting clot formation. Westein and colleagues⁸ patterned collagen in a striped pattern to compare the deposition of platelets and VWF at points upstream, within, and downstream of the stenosis region. In this device, platelet aggregation was enhanced in the stenotic outlet regions at 60%–80% occlusion over a range of inlet wall shear rates. Nesbitt and colleagues⁷ used a fully collagen-coated stenosis microfluidic device to study the localization of platelets in low-shear zones at the downstream face of forming thrombi. They found that soluble agonists were not required for this aggregation in response to shear microgradients, which reinforces the crucial role that VWF plays in thrombus formation following high shear stenoses.

Li and colleagues⁹ also utilized a stenotic microfluidic device with a couple key difference in device scale and thrombotic surface placement. The stenotic channel was much larger than in the previously discussed stenosis devices, with a 750 μm channel tapering to 250 μm . This matches more closely with pathologically relevant eccentric constriction or stenosis but requires the use of large volumes of blood, which reduces applicability to point-of-care diagnostic devices. Second, the full channel of the device was coated with collagen instead of localizing the thrombotic surface to patterned strips on the glass surface. However, they did not observe any platelet clotting upstream or downstream of the stenosis region, enabling it to be used for a highly systematic and systemic analysis of the effect of aspirin (ASA) and eptifibatid (GPIIb/IIIa inhibitor) on occlusive thrombosis and thrombus stability across a range of high shear rates.

In this study, it was found that shear rates have significant effects on both occlusion time/dose-response curves for both therapies. For example, ASA had very little effect on high shear occlusion times, while eptifibatid was able to reduce occlusion and increased efficacy with dose at all shear rates tested. It was also found that high shear thrombi formed in the presence of ASA were 4 times more likely to detach than either untreated or eptifibatid-treated controls. This and similar microfluidic devices that evaluate the efficacy of antiplatelet therapies in a wide range of shear rates are valuable to optimizing treatment models for high shear thrombotic diseases.

Impingement-post device

Herbig and Diamond designed an impingement-post microfluidic device that utilized fluid shear control to study fibrous VWF mechanobiology and biochemistry in flow.¹⁰ Similar to the stenosis device, the inlet channel narrowed rapidly from 250 μm to 60 μm to increase shear and elongational forces in the EDTA-anticoagulated PFP to promote VWF aggregation into fibers. This device, however, contained a 30 μm micropost (rather than a collagen surface) in the middle of the channel to capture VWF fibers aggregated in the shear flow. This allowed the study of aggregated plasma VWF fibers without potentially confounding collagen present [Fig. 2(a)]. After VWF fibers had been formed and captured on the micropost, the perfused fluid could be

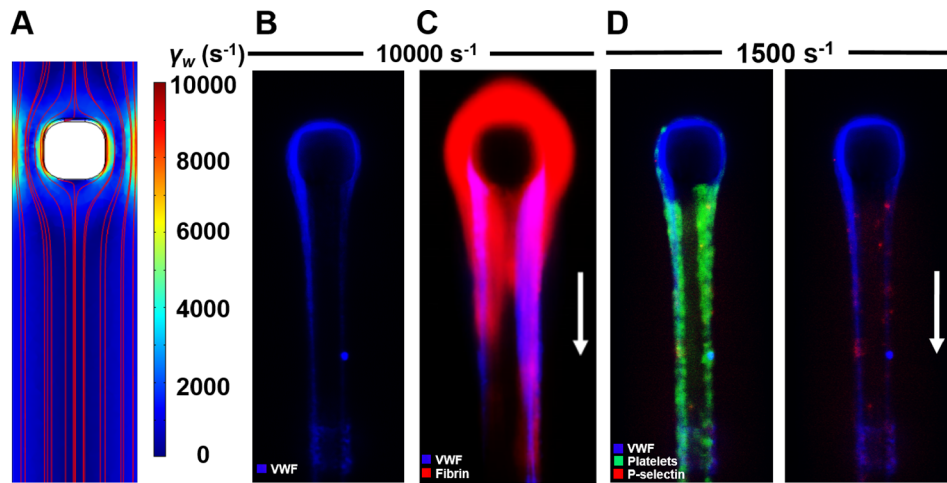


FIG. 2. Impingement-post microfluidic device enables the study of coagulation and platelets on fibrous VWF. (a) COMSOL simulation shows the increased shear rate around the micropost even at relatively low inlet shear rates ($1000 s^{-1}$). (b) EDTA-anticoagulated PFP was perfused at inlet shear rates of $>5000 s^{-1}$, resulting in the formation of VWF fibers upstream, which hatch on the micropost and are held there by fluid forces. (c) Following VWF fiber formation, coagulable PFP was perfused over the VWF fiber, resulting in local fibrin formation. (d) When PPACK/Apixaban-inhibited WB was perfused over already formed VWF fibers, platelets rolled and firmly adhered to the VWF surface, resulting in some shear-induced platelet activation, as marked by P-selectin.

changed to study proteolytic activity on VWF, coagulation on VWF, or platelet/VWF interactions in low and high shear environments.

VWF fibers formed in the impingement-post microfluidic device were aggregated from EDTA-anticoagulated plasma VWF that had already been processed by ADAMTS13 in circulation, which makes the fibers distinct from the unprocessed ultra-large VWF (ULVWF) released from stimulated endothelial cells. The size of the VWF fibers captured in this device increased with increasing wall shear rates above $5000 s^{-1}$ in the narrowed channel [Fig. 2(b)]. These fibers were found to be resistant to cleavage by ADAMTS13 and tissue plasminogen activator but were cleaved by plasmin. Although ADAMTS13 cleaves ULVWF, the aggregated VWF that makes up the fibers has already been processed by the protease in plasma circulation, and so, any additional proteolytic activity does not have an effect on the fiber. This finding may suggest the clinical implication that protease selection for cleaving VWF in thrombolytic situations will vary based on whether the VWF in the clot is primarily endothelial released ULVWF or shear-induced VWF fibers from plasma. In high shear thrombotic situations, ADAMTS13 may be ineffective due to the resistance of plasma VWF aggregated in these clots due to the high shear flow environment.

Coagulation on VWF fibers was also examined by forming VWF fibers from EDTA-anticoagulated PFP with and without active coagulation factors present and then perfusing coagulable PFP over the fibers to observe fibrin formation on the VWF surface. It was observed that the coagulation factor complex assembly and full intrinsic coagulation were possible on the surface of VWF fibers alone, as evidenced by fibrin polymerization on the VWF surface [Fig. 2(c)]. Interestingly, when VWF fibers were fluorescently labeled for FXII(a), it was strongly colocalized in the VWF. Additionally, when the VWF fibers were formed with FXII-deficient PFP and the coagulable PFP was perfused over, no fibrin formed. This was evidence that coagulation factors trapped in the aggregated VWF can lead to coagulation on the VWF fiber surface, potentially exacerbating thrombosis in extreme shear areas.

The adhesion and activation of platelets on fibrous VWF were also examined in this device. After VWF fibers had been formed by shearing thrombin- and FXa-inhibited PFP, similarly inhibited whole blood was perfused over the fibers at $1500 s^{-1}$ and $3000 s^{-1}$. Platelets both rolled and stably adhered to the VWF fibers using both GPIb and $\alpha_{IIb}\beta_3$, as previously observed in ULVWF.¹¹ Activation of the stably adhered platelets was also observed in a

shear-dependent manner, using P-selectin as a marker of platelet activation [Fig. 2(d)]. This shear-induced platelet activation (SIPA) may be important in the extreme flows around a nearly occlusive thrombus, where VWF/platelet interactions may lead to full occlusion.

This impingement-post microfluidic device design was later used by the Lopez group¹² to examine the effect of ADAMTS13-processed small VWF fragments on VWF fiber aggregation in both purified systems and patient samples. To create the small VWF fragments, purified plasma VWF was incubated with recombinant ADAMTS13 in urea to cleave the VWF multimers, before purifying them out of the solution. These multimers were then doped into plasma and were found to reduce the size of VWF fibers formed. These VWF fibers were more pronounced than those formed by thrombotic thrombocytopenic purpura (TTP) and von Willebrand disease (VWD) 2A patient plasma. This suggests that the hemostatic defect associated with VWF 2A is the result of the presence of excessive quantities of VWF fragments in addition to the deficiency of large multimers, and the thrombotic phenotype of TTP results from the deficiency of smaller fragments in addition to the excess presence of ULVWF.

CONTROL OF FLOW GEOMETRY

Pathological flows occur in regions of the body with 3-dimensional geometry, including at stenoses and bifurcations and within thrombi. Microfluidics can recapitulate elements of these geometries to better understand clotting in pathological flows. Biomimetic stenoses, stagnation point geometries, and pathologic interstitial flow all have been studied using microfluidics.

Biomimetic stenosed channels

One common criticism of traditional square microfluidic channels is that they do not fully replicate the flow patterns found in round blood vessels. To address this, some groups have used a cylindrical piece of material that PDMS can cure around, which can then be removed to leave behind a cylindrical-shaped microchannel. Mannino and colleagues¹³ used a 500 μm diameter optical fiber as their cylindrical mold, which they modified to create the flow geometry of interest. To create a stenosis, a razor blade covered with fine sandpaper was used to sand a fine notch out of the optical fiber, resulting in the creation of a stenosis in the final PDMS device. Costa and colleagues¹⁴ utilized 3D-printing to recapitulate the 3D vessel geometry and local blood flow patterns in a microfluidic device. Although these devices do not fully recapitulate the 3D flow found in larger blood vessels due to the low Reynolds number nature of microfluidics, the round channels provide flow conditions more similar to the blood vessels than square channels can.

Using computed tomography angiography data of a coronary artery, both healthy and stenosis models of the vessel were 3D printed and used as a template for PDMS-based soft lithography. The resulting channels were seeded with human umbilical vein endothelial cells to form a confluent monolayer. When recalcified citrated WB was perfused through the channels at an upstream wall shear rate of 1000 s^{-1} , the healthy geometry did not show any sign of thrombosis along the length of the channel for 15 min. Both the stenotic geometries (55% and 67% occlusion) displayed thrombosis in the downstream portion of the stenosis beginning at 2 min, with significant platelet aggregation in the recirculation zone. Because shear rates in the stenosis reached $>10\,000 \text{ s}^{-1}$, VWF also likely played a role in recruiting platelets to the thrombus. The innovative combination of 3D printing and traditional PDMS-based soft lithography demonstrated how 3D hemodynamics can be studied using microfluidic techniques.

Stagnation point device

Because pathological flows often involve recirculation, stagnation points are an important part of thrombosis downstream of stenoses. A novel microfluidic flow geometry was also used by Herbig and colleagues¹⁵ to examine the effect of stagnation point flow on thrombosis. The microfluidic device was designed such that an inlet channel would perfuse whole blood perpendicularly to a fibrillar collagen/TF thrombotic surface before being diverted away parallel to

that surface, resulting in a stagnation point [Figs. 3(a) and 3(b)]. Because clot growth could be observed from the side, labeling platelets, P-selectin, fibrin, and VWF enabled the observation of the overall structure of the clot and how it varied across different conditions.

Thrombi formed in stagnation point flows at both low and high inlet flow rates exhibited a core-shell architecture [Fig. 3(c)] with a dense P-selectin-positive core surrounded by a more diffuse P-selectin-negative shell, as previously described for parallel flow thrombus formation.¹⁶ The overall shape of the thrombi varied with the inlet flow rate, with a more dendritic structure at low shear rates and a more compact and even structure at high shear rates. VWF was present throughout the thrombi formed at 10 and 100 $\mu\text{l}/\text{min}$, but when N-acetylcysteine (NAC), an FDA-approved drug, was added to blood, the resulting thrombi were smaller at 10 $\mu\text{l}/\text{min}$ and failed to accumulate at 100 $\mu\text{l}/\text{min}$ [Fig. 3(d)]. This result was consistent with previous work demonstrating the ability of NAC to interfere with VWF/platelet interactions and suggests the importance of VWF to clot stability in this geometry.¹⁷ In contrast, when fibrin polymerization was blocked with Gly-Pro-Arg-Pro (GPRP), the thrombi were able to stably grow to the same size, suggesting that fibrin is not required for clot stability in stagnation point flows.

This device design led to two main advantages over previous stagnation point studies. One advantage was that, in contrast to previous radial flow studies, this device created an essentially two-dimensional flow, which is more similar to the flow and transport found in stenosed blood vessels around stagnation points. Another advantage was the side-view orientation of the clotting region in the device. Since the structure and content of clots vary along their height, this device was able to detect spatial differences such as VWF incorporation and P-selectin activation. Although not recapitulating the high Reynolds number flows found arterial stagnation flows, this strategy of microfluidic device design, with localized thrombotic regions located on a side wall, may allow for important comparisons between well-controlled flow and biochemical conditions *in vitro* and more complex and physiological *in vivo* intravital mouse imaging.

Shear-induced NETosis

During the early stages of thrombosis, clot growth is regulated by the wall shear rate and the wall shear stress, whereas interstitial flow through thrombi described by Darcy's law only plays a minor role. However, as clots become occlusive, permeation becomes a major player in the transport of solute and fluid especially under large trans-thrombus pressure drops.¹⁸ In

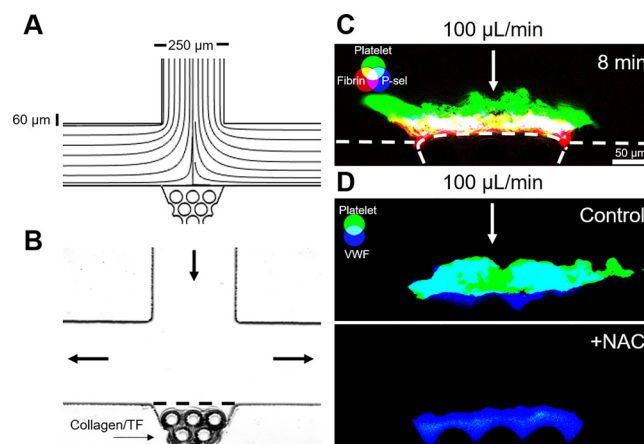


FIG. 3. Stagnation point microfluidic device demonstrates the core-shell and VWF-dependent thrombus architecture. (a) COMSOL simulation streamline diagram confirms a stagnation point at the center of the collagen scaffold region. (b) Collagen/TF was loaded into the scaffold to create a thrombotic surface that could be observed from the side. (c) CTI-anticoagulated WB was perfused through the device at an inlet flow rate of 100 $\mu\text{l}/\text{min}$ (wall shear rate, 1000 s^{-1}). The resulting thrombi exhibited a core-shell architecture, with a fibrin-rich and P-selectin-positive core, and a P-selectin-negative platelet shell. (d) Thrombi formed with CTI-anticoagulated WB formed VWF-rich thrombi. Addition of 30 mM N-acetylcysteine (NAC) eliminated platelet deposition at high shear rates.

addition, blood cells within the clots respond to high hemodynamic forces through SIPA¹⁹ and the release of neutrophil extracellular traps (NETs).²⁰

Yu *et al.* used an 8-channel microfluidic device [Fig. 4(a)] to investigate the effect of hemodynamic forces on neutrophils within sterile occlusive thrombi. The pairing of clot forming channels with pressure relief channels (using EDTA treated whole blood) makes this *in vitro* thrombosis model more physiological by setting a limit on the trans-thrombus pressure drop. Clots formed at arterial shear rates contained significantly more extracellular DNA [Fig. 4(b)] than the ones formed at venous shear rates both in the presence and absence of thrombin generation. The ease of flow manipulation enabled abrupt flow shift-up from venous to arterial conditions, revealing the strong temporal coupling between the onset of NET release and high hemodynamic forces. For an occlusive clot 1 mm in length, a pressure drop of >87 mm Hg (or an initial shear rate of 500 s^{-1}) was found to be sufficient to drive NET generation. A numerical simulation of interstitial flow through a platelet clot was used to calculate the forces on a deformable neutrophil. The peak fluid shear stress reached 15 Pa [Fig. 4(c)], the lytic threshold for neutrophils in a cone-and-plate viscometer. Sustained high hemodynamic forces also led to significant deformation and membrane stress on the neutrophil [Fig. 4(d)]. In humans, venous thrombi are usually millimeters long with a pressure drop per unit length much smaller than the shear-induced NETosis threshold. In contrast, arterial and arteriolar thrombi can have pressure gradients large enough to drive NET generation depending on the clot length.

CONCLUSIONS AND FUTURE WORK

As demonstrated in this review, microfluidics provides a powerful technique for studying pathological blood flows and their role in thrombosis. The iterable design and ease of

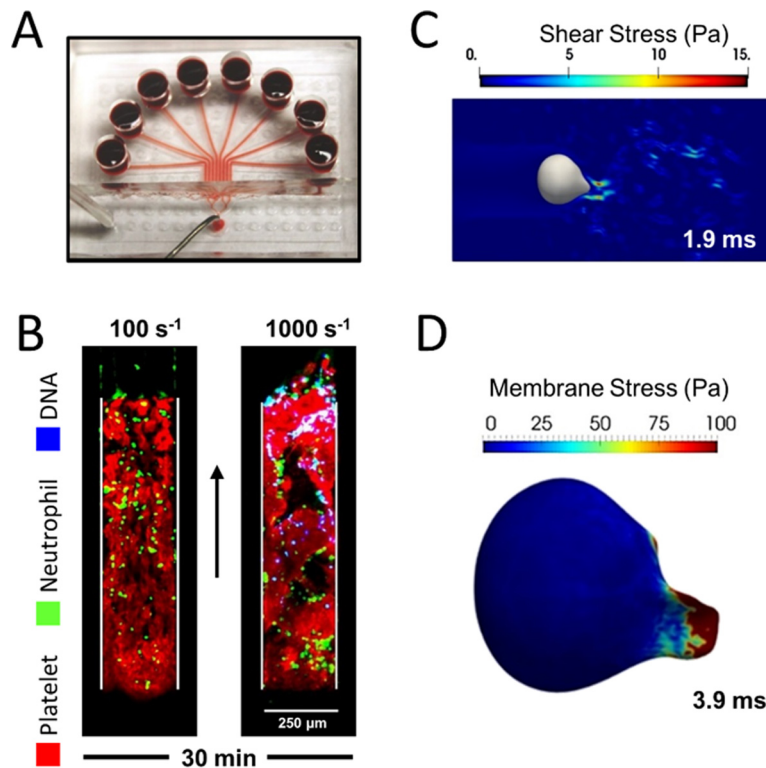


FIG. 4. Hemodynamic force drives rapid NETosis within sterile occlusive thrombi. (a) PPACK/CTI treated whole blood was perfused over collagen/TF surfaces in an 8-channel microfluidic device. (b) An initial arterial wall shear rate of 1000 s^{-1} in the pressure-relief mode resulted in rapid NET generation. (c) Simulation of flow across an occlusive thrombus under a pressure gradient of 70 mm Hg/mm-clot calculated the peak fluid shear stress at 1.9 ms to be 15 Pa . (d) The pressure gradient resulted in significant deformation and membrane stress on the physically entrapped neutrophil at 3.9 ms (arrow: flow direction).

fabrication enable rapid adjustment in response to new results, and small required blood volumes reduce the costs necessary for each new experiment. The tight control over blood biochemistry, flow conditions, and channel geometry are useful to recapitulate the hemodynamic conditions found in relevant diseases.

However, there are also significant limitations to microfluidic devices for hemodynamic research. The small length scale of microfluidic channels creates low Reynolds number (Re) flows that do not match pathological flows in coronary artery stenosis. With microfluidics, it is difficult to obtain boundary layer separation and reattachment in order to create a recirculation vortex distal of a stenosis, which is typical of a higher Re flow. Additionally, few studies have created and validated pulsatile flows in microfluidic devices.

There are certain gaps in microfluidic studies with pathological blood flows. Much of the work has focused on thrombosis using healthy blood. The use of patient blood could provide a valuable opportunity for disease-specific blood phenotyping. Toward exploring disease states, Jain *et al.*²¹ created a microfluidic device with a network of stenosed channels to study the clotting time of blood using porcine blood *ex vivo* following endotoxemia and heparin therapy. Dimasi and colleagues²² designed a high shear microfluidic device that simulates the shear stress profiles of ventricular assist devices. The translation of microfluidic technology from the research bench to clinical diagnostic applications presents a future opportunity for the field.

ACKNOWLEDGMENTS

This work was supported by NIH predoctoral training Grants 5T32HL007954-15 (B.A.H.) and NIH R01 HL103419 (S.L.D.).

- ¹D. E. McMillan, *Stroke* **16**, 582 (1985).
- ²R. S. Kane, S. Takayama, E. Ostuni, D. E. Ingber, and G. M. Whitesides, *Biomaterials* **20**, 2363 (1999).
- ³K. J. Regehr, M. Domenech, J. T. Koepsel, K. C. Carver, S. J. Ellison-Zelski, W. L. Murphy, L. A. Schuler, E. T. Alarid, and D. J. Beebe, *Lab Chip* **9**, 2132 (2009).
- ⁴R. W. Muthard and S. L. Diamond, *Biorheology* **51**, 227 (2014).
- ⁵S. Nomura, H. Nagata, K. Oda, T. Kokawa, and K. Yasunaga, *Thromb. Res.* **47**, 47 (1987).
- ⁶T. V. Colace and S. L. Diamond, *Arterioscler., Thromb., Vasc. Biol.* **33**, 105 (2013).
- ⁷W. S. Nesbitt, E. Westein, F. J. Tovar-Lopez, E. Tolouei, A. Mitchell, J. Fu, J. Carberry, A. Fouras, and S. P. Jackson, *Nat. Med.* **15**, 665 (2009).
- ⁸E. Westein, A. D. van der Meer, M. J. E. Kuijpers, J.-P. Frimat, A. van den Berg, and J. W. M. Heemskerk, *Proc. Natl. Acad. Sci. U.S.A.* **110**, 1357 (2013).
- ⁹M. Li, N. A. Hotaling, D. N. Ku, and C. R. Forest, *PLoS One* **9**, e82493 (2014).
- ¹⁰B. A. Herbig and S. L. Diamond, *J. Thromb. Haemostasis* **13**, 1699 (2015).
- ¹¹B. J. Fredrickson, J. F. Dong, L. V. McIntire, and J. A. López, *Blood* **92**, 3684 (1998).
- ¹²S. Feghhi, A. St. John, J. Harris, J. Le, D. W. Chung, J. Chen, and J. A. Lopez, *Blood* **128**, 3718 (2016).
- ¹³R. G. Mannino, D. R. Myers, B. Ahn, Y. Wang, M. Rollins, H. Gole, A. S. Lin, R. E. Guldberg, D. P. Giddens, L. H. Timmins, and W. a. Lam, *Sci. Rep.* **5**, 12401 (2015).
- ¹⁴P. F. Costa, H. J. Albers, J. E. A. Linssen, H. H. T. Middelkamp, L. van der Hout, R. Passier, A. van den Berg, J. Malda, and A. D. van der Meer, *Lab Chip* **17**, 2785 (2017).
- ¹⁵B. A. Herbig and S. L. Diamond, *Cell. Mol. Bioeng.* **10**, 515 (2017).
- ¹⁶T. J. Stalker, E. A. Traxler, J. Wu, K. M. Wannemacher, S. L. Cermignano, R. Voronov, S. L. Diamond, and L. F. Brass, *Blood* **121**, 1875 (2013).
- ¹⁷S. Martinez de Lizarrondo, C. Gakuba, B. A. Herbig, Y. Repessé, C. Ali, C. V. Denis, P. J. Lenting, E. Touzé, S. L. Diamond, D. Vivien, and M. Gauberti, *Circulation* **136**, 646 (2017).
- ¹⁸A. L. Fogelson and K. B. Neeves, *Annu. Rev. Fluid Mech.* **47**, 377 (2015).
- ¹⁹J. R. O'Brien, *Lancet* **335**, 711 (1990).
- ²⁰X. Yu, J. Tan, and S. L. Diamond, *J. Thromb. Haemost.* **16**, 316–329 (2017).
- ²¹A. Jain, A. Graveline, A. Waterhouse, A. Vernet, R. Flaumenhaft, and D. E. Ingber, *Nat. Commun.* **7**, 10176 (2016).
- ²²A. Dimasi, M. Rasponi, J. Sheriff, W.-C. Chiu, D. Bluestein, P. L. Tran, M. J. Slepian, and A. Redaelli, *Biomed. Microdevices* **17**, 117 (2015).